A 3-D Printed Microfluidic Device Enabling Efficient Bioparticle Conjugation in Biological Assays

Muhammad Nabeel Tahir
Department of Electrical Engineering
Rutgers the State University of New Jersey
Piscataway, USA
nabeel.tahir@rutgers.edu

Brandon K Ashley
Department of Biomedical Engineering
Rutgers the State University of New Jersey
Piscataway, USA
bka32@scarletmail.rutgers.edu

Umer Hassan
Department of Electrical Engineering
Rutgers the State University of New Jersey
Piscataway, USA
umer.hassan@rutgers.edu

2024 46th Annual International Conference of the IEEE Engineering in Medicine and Biology Society (EMBC) | 979-8-3503-7149-9/24/$31.00 ©2024 IEEE | DOI: 10.1109/EMBC53108.2024.10782751

***Abstract*— Conjugating a micro/nanoparticle with the biomolecule has proved useful in diagnosing complex diseases (cancer/sepsis). The properties of the conjugating particle help in quantifying, enumerating, and detecting the target species. The conjugation technique has found its applications in diagnostics and therapy, biosensing, and sorting. The major drawback of state-of-the-art conjugation techniques is that they are time-consuming and labor-intensive. One possible solution to the problem posed by the existing conjugation technique is to use microfluidic devices. Microfluidic devices with their precise control, variable geometry, high mixing, and mass transfer efficiencies are widely used in fluid mixing applications. 3D-printed microfluidic devices have been used to study the conjugation of particles and the detection of different cells in many state-of-the-art studies. In this study, a planer 3D printed micromixer with multiple serpentine channels was developed. The performance of the device was evaluated by performing numerical simulations and running the fluids at various flow rates through the serpentine channels. The numerical simulations produced a fluidic mixing index of ~0.96 at various mesh configurations. Similar particle conjugation efficiency was achieved in just ~3-5 minutes as compared to hours of incubation with state-of-the-art conjugation protocols.**

Keywords—Conjugation, 3D printing, COMSOL, Mixing Index.

I. Introduction

Particle or antibody conjugation has played an important role in the field of bioscience and healthcare with applications in disease diagnostics and therapeutics [1], [2]. In diagnostics, conjugation is used for targeted detection and isolation of biomolecules where fluorescent or magnetic micro/nanoparticles are attached to the antibodies [3], [4]. In therapeutics, conjugation facilitates the delivery of therapeutic biomolecules to targeted cells or tissues by binding them to micro/nanoparticles or liposomes. Although micro/nanoparticle conjugation offers many advantages, the preparation involves many challenges. It involves various steps, regular incubation for hours, and labor-intensive and time-consuming processes. Moreover, the batch production of these conjugated particles often suffers from reproducibility errors and quality [5]. Thus, increasing the overall production cost and time required to prepare good-quality samples. To address these challenges notable techniques have been developed and employed out of which microfluidics stand out the most.

Microfluidics is an interdisciplinary field of research in science and technology that manipulates fluids on microliters and nanoliter scales, within a channel ranging from a few micrometers to hundreds of micrometers [6], serves as a bridge between engineering, biochemistry, biotechnology, healthcare, and physics. During the past few decades, groundbreaking developments in the field of microfluidics have transformed the various fields of science and introduced new approaches that are being used in developing disease diagnostic and drug delivery systems, material synthesis, and environmental analysis. At these small scales, the laminar flow [7] is one of the greatest challenges that affect the efficiency of microfluidic devices. At laminar flow, the fluid has a very low Reynolds number. A low Reynolds number specifies that two fluids flowing side by side will not mix efficiently until some external mechanism is employed to support the mixing process. The microfluidic devices that are designed for disease diagnosis and drug discovery where the interaction of microparticles or cells in the fluid is critical a laminar flow poses a grave challenge. Significant efforts have been made to mitigate this challenge by the research community using either passive or active mixing. Active micro-mixing often integrates external devices e.g. periodic electric osmotic flow generators [8], thermal actuators [9], [10], ultrasonic transducers [11], [12], and dielectrophoretic magnetohydrodynamic flow generators [13] into the channel. However, adding these external devices to the channel complicates the fabrication process and adds new challenges e.g., heat generation and power consumption. Therefore, there is a constant need to design a passive micromixer.

A passive micromixer does not rely on external sources to achieve effective mixing but rather uses the intrinsic properties of the fluids and the geometries of the channel. The mixing efficiency is improved either by using 2D channels or complex 3D structures that increase the contact area between two or more mixing species. 3D micromixers incorporate multiple splitting, spiral, and recombining channels into a 3D structure [14] to increase the mixing efficiency. The researchers also developed embedded barriers and interconnected barriers inside the 3D structures to improve the mixing indices [15]. A 3D micromixer fabrication requires multiple steps of lithography, or if these devices are 3D printed, they end up using a huge amount of printing material and time required thus limiting their use. Several researchers have employed the serpentine geometry to acquire similar mixing efficiencies as with the 3D micromixer but with a 2D design [16], [17]. A serpentine mixer, which can be characterized by the sinus or winding channels is among the prominent solutions that have emerged from the decades of research on developing an efficient micromixer in a laminar flow regime. The serpentine geometry forces the fluid streamlines to continuously diverge and converge, resulting in a uniform and enhanced mixing.

This study aimed to use serpentine geometry to design, develop, and fabricate the micromixer as an assistive device

for bioparticle conjugation. We benefitted from the latest advancements in 3D printing technology and fabricated a micromixer with multiple serpentine channels. To study the mixing capabilities of the designed structure numerical simulations were performed using COMSOL. And an extensive experimental procedure was employed to quantify the mixing index and particle conjugation efficiency of the device. The results form numerical simulations and experimental setup were compiled and compared with the results obtained from a control experiment.

II. Methods and Materials

A. Device Design and Numerical Simulations

The device used in this study was designed using the CAD software contain 40 serpentine channels, each channel has the same dimensions of 5mm × 1mm × 1mm joined a circular joint with diameter of 1mm. The device was printed using liquid SLA based 3D-printer. Numerical fluid dynamics simulations were performed using COMOSL 6.1 to estimate the velocity flow field and mixing efficiency of the device using the same CAD design. The computational geometry of the serpentine mixer was simulated by dividing it into ~29,438-77,902 small finite elements using the meshing feature of COMSOL. Meshing discretizes the computational domain into smaller cells where the governing Navier Stokes equations are optimized. The physics models selected in COMSOL to simulate the device included the creeping flow and transport of diluted species. The two inlets of the device are set to contain Newtonian fluids with a density and viscosity of 1000 Kg/m^3, and 1 mPa s, respectively. The concentration of the fluids at inlet 1 was set to C1=1 mM, and at inlet 2 to C2= 0 mM. The feeding flow rate, Q, into both inlets was independent and was set to 15 µL/min resulting in the total flow rate of 30 µL/min and simulations were performed. The resulting concentration profile of the fluids flowing through Inlet 1 and Inlet 2 was then used to measure the mixing efficiency of the device using the standard formula discussed in [14]. To generate the mixing efficiency a 2D plane was drawn on in yz plane at 40 fixed locations on the serpentine mixer and concentration data was extracted to generate the mixing index value at each location. To minimize selection bias and better estimate the mixing index the planes were selected on the rectangular straight channels of the serpentine mixer. The final mixing index value at each location is calculated using the equation:

$$MI = 1 - \frac{1}{\mu_c}\sqrt{\frac{\sum_{i=1}^{N}(c_i-\mu_c)^2}{N}} \qquad 1)$$

For each plane drawn on a specific location on the yz, plane the μ_c represents the mean concentration, c_i represents the instantaneous concentration, and N represents the total number of points in that 2D plane.

B. Sample Preparation

To perform the mixing experiments the polystyrene particles of size 10µm coated with streptavidin (Product # SVP-100-4) and 3.4 µm coated with biotin (Product # TP-30-5) were procured from Spherotech Inc. Initially, the concentrated solutions of microparticles were sonicated for 20 minutes each before preparing the two different stock solutions of 10µm and 3.4µm particles. A 2mL solution of each particle solution and 1783µL of the 1x PBS solution. The 10µm particles were diluted down to 3×10^5 particles/mL and 3.43µm particles were diluted down to

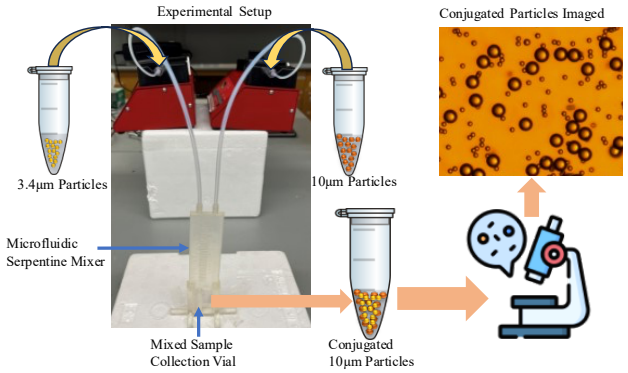

Figure 1: The flow chart showing the experimental setup, sample preparation, and imaging protocol.

1.92×10^7 particles/mL in the final mixed solution 4mL. Finally, the prepared separate solutions of 10µm and 3.4µm particles were vortexed for 30s before loading into the syringes for mixing experiments.

C. Control Experiment

To study the effect of microfluidic mixing and to draw a fair comparison with the traditional incubation-based conjugation protocols the control experiment was conducted. Twelve stock solutions of each 10 µm and 3.4µm particles were prepared following the sample preparation protocol discussed above. These 2mL solutions were mixed to finally prepare the 12 4mL solutions. The solutions were then incubated in a refrigerator. After one hour of incubation, one sample was taken out vortexed for one minute, and then imaged using a camera attached to the microscope. The complete control experiment spanned for 12 hours where one sample was being imaged after the gap of one hour. In total twelve samples generated 12 experimental data that could be analyzed to study the particle conjugation over the span of 12 hours.

D. Mixing Experimental Setup and Data Collection

The stock solutions of both 10µm and 3µm particles were loaded into two separate syringes and were attached to two syringe pumps. The tubes with an inner diameter of 1.6mm and a needle with an outer diameter of 1.6mm connected the syringes to device inlets. A custom-designed 3D-printed platform holds the device and sample collection vial. To completely understand the effect of microfluidic channels on the conjugation efficiency of micro/nanobeads both syringe pumps were set to three flow rates of 15, 20, and 30µL/min three mixing experiments were performed independently at

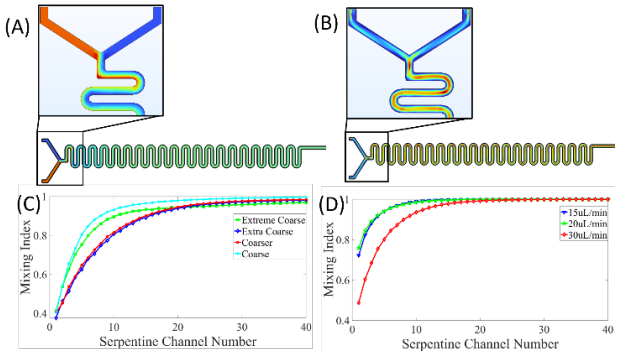

Figure 2: Simulation Results. (A) Concentration profile of simulation of species 1(mol/m^3). (B) Velocity profile of serpentine mixer. (C) Mixing efficiency of the serpentine mixer. (D) Mixing efficiency of the serpentine mixer at 15uL/min, 20uL/min, and 30uL/min flow rates.

each flow rate. When mixed the fluids inside the microfluidic channel resulted in a combined flow rate of 30, 40, and 60µL/min. Figure 1 shows the experimental setup used to perform all the mixing experiments. To quantify the efficiency of the mixing device, a 0.5µL sample was collected from the outlet of the mixing device. The sample was placed in a 96-well plate and left for approximately 10 minutes for the beads to settle at the bottom of the well. The entire drop was imaged using a camera attached to Olympus IX81 microscope. Depending on the number of beads a total of 8-10 images were collected for each drop. The images were saved and later used to analyze the conjugation efficiency.

E. Data Analysis and Processing

The data collected from each drop was manually analyzed to count the number of 3µm beads conjugated with the 10µm beads. First, all 10µm were counted in the image. Then the number of 10µm beads with one, two, three, or more 3µm beads conjugated were counted. A dataset has been generated containing the number of total 10µm beads and conjugated 3µm beads for each image and each experiment performed. The conjugation efficiency of the beads was calculated for each image using equation 2. The average conjugation efficiency and average number of 10µm beads were calculated for all four independent experiments performed for each flow rate and the resulting graphs were generated.

$$CE = \frac{1}{M}\sum_{M}\frac{\tilde{X}}{X} \times 100 \qquad 2)$$

Where CE is the conjugation efficiency, M is the total number of experiments performed at each flow rate, $\tilde{X}$ is the number of cconjugated10µm beads while, X is the total number of 10µm beads collected.

III. Results and Discussion

A. Numerical Simulation Analysis

The concentration profiles evaluated using the COMSOL simulations were used to estimate the mixing index values at the selected points on the serpentine channels using the equation (1). The mixing index at the selected points on the serpentine mixer was evaluated for four different meshing configurations, i.e., extreme coarse (29,438 cells), extra course (43,751 cells), courser (51,498 cells), and coarse (77,902 cells) to study the effect of changing the mesh size. Figure 2 (C) shows the mixing index plots of all the mesh configurations simulated in COMSOL. The mixing index varies from 0 to 1 where the value zero represents no mixing while the value one represents the complete mixing of the two species in the microfluidic channel. The mixing index itself is an alias of the mixing efficiency of the microfluidic serpentine mixer and is interchangeably used. It can be observed from Figure 2 (C) that at a lower number of serpentine channels and even at the extreme coarse mesh configurations the serpentine mixer has a mixing index or efficiency closer to 90%. The extreme coarse and coarse mesh configurations depict a mixing efficiency of above 90% at the 15th serpentine channel while the extra coarse and coarser mesh configurations have a mixing efficiency slightly lower than 90%. This could be justified by the fact that the convergence of the finite elements method to lower error rates in the cells of the first 15 channels is not as efficient as in extreme coarse and coarse simulations. But as the simulations progress the average mixing efficiency in any mesh configuration reaches 98% or above as can be observed by the vertical line drawn at the 30th serpentine channel. This also shows that by the time both species arrive at the 30th serpentine channel 98% of the concentrations have already been mixed. Although increasing the number of discretized cells in the mesh configurations provides a better estimate of the mixing index as the efficiency is increased due to convergence of the finite element method but the overall difference in the efficiencies is not significant amongst the mesh configurations. Therefore, it can be inferred from the results that the mixing index or efficiency is independent of the meshing configurations. Moreover, increasing the number of cells in the mesh configuration also increases the simulation time and requires more efficient and powerful computational resources therefore the extreme coarse mesh configurations can be used to evaluate the performance of the serpentine mixer.

The mixing efficiency of the serpentine mixer was also evaluated at the higher flow rates to understand the effect of the flow rate on the mixing index. By setting the mesh configuration to extra coarse the simulations were generated at flow rates of 30µL/min, 40µL/min, and 60µL/min. The mixing index plots were created using the concentration profile data obtained as shown in Fig. 2(D). The 60µL/min flow rate exhibited a lower mixing efficiency as compared to the other flow rates. At 40µL/min and 30µL/min flow rates the mixing index values are significantly higher than the 60µL/min flow rate. This could be attributed to the fact that at these flow rates, the simulations converge to global minima. Apart from the mixing index results the concentration profiles of species 1 and the velocity profiles were generated using the COMSOL and plotted in Fig. 2 (A) and Fig. 2 (B) respectively.

B. Experimental Results

The data collected from the mixing experiments performed according to the protocol discussed in section II-D was used to analyze the performance of the serpentine mixer. To quantify the performance of the experimental setup a new metric called conjugation efficiency was evaluated using equation 2. A maximum conjugation efficiency of 28% was achieved using the serpentine mixer at a flow rate of

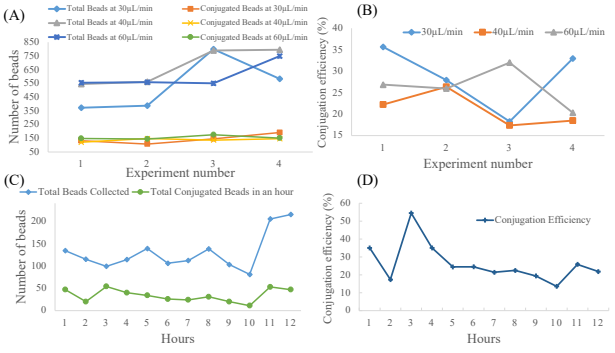

Figure 3: Experimental data and results. (A) Total collected and conjugated beads at 30µL/min, 40µL/min, and 60µL/min. (B) Conjugation efficiency at 30µL/min, 40µL/min, and 60µL/min. (C) Total collected and conjugated beads for control experiment at each hour. (D) Conjugation efficiency of control experiment at each hour.

30µL/min. While the control experiments and the experiments done at 40µL/min and 60µL/min resulted in an average conjugation efficiency of 26%. Fig. 3(A) shows the average number of total beads/microparticles collected in each experiment at a specific flow rate and the average number of conjugated particles, while Fig. 3(B) shows the conjugation efficiency obtained during each experiment.

Similarly, Fig. 3(C) shows the total number of beads collected and conjugated at each hour of the control experiment and Fig. 3(D) shows the conjugation efficiency of the control experiment. The lower conjugation efficiency at higher flow rates can be associated with less interaction between the microparticles or the limited time allowed for particles to bind to each other. While at a slower flow rate, the particles have sufficient time to bind to each other and hence have a higher conjugation efficiency. The control experiment shows higher conjugation efficiency during the first 3 hours of incubation while the accuracy drops as the incubation time increases. This results in the average conjugation efficiency close to the one achieved by the serpentine mixer. Although the difference between the average conjugation efficiency of control experiments and the average efficiency of serpentine mixers is not significant, the most important factor to be considered is the time reduction. With a serpentine mixer, the average time to perform an experiment even at a lower flow rate is approximately ~3-5 minutes which is significantly lower than control experiments where the sample is required to be incubated for hours. Therefore, the serpentine mixer can be effectively used as an alternative to the state-of-the-art control experiment to achieve the conjugation of micro particles with similar conjugation efficiency but reduced processing time.

IV. Conclusion

A 3D printed 40 channel microfluidic serpentine mixer was employed to facilitate the micro/nanoparticle conjugation. Microfluidic devices and systems have the potential to revolutionize the various fields of science, especially bioscience. Using design, experimentation, and numerical simulations a deeper understanding of microfluidic mixing and particle conjugation has been developed. The experimental results have shown that the serpentine micromixers are not only equally capable but efficient enough to conjugate the microparticles as the conventional techniques. The conjugation efficiency of 28% as compared with the standard incubation-based conjugation technique suggests that the serpentine micromixer can achieve similar results but with significant reduction in experiment time. Moreover, the COMSOL based numerical simulations that evaluate the mixing efficiency of the device further strengthen the claim than the 3D printed microfluidic device can be effectively used an alternative to stat-of-the-art particle conjugation techniques. Although significant strides have been made to optimize the performance of micromixer yet there is huge room for improvements. The challenges posed by limitations of 3D printing technology further makes it possible to develop and fabricate the low-cost device with submicron level resolution as at this state the particle conjugation process can expedited exponentially. In future work we aim to explore the various geometric modifications in the serpentine micromixer that improve the particle conjugation and overall performance of micromixer.

Acknowledgment

The Authors would like to acknowledge the funding support from National Science Foundation (Award # 2002511), Department of Electrical and Computer Engineering, and Global Health Institute at Rutgers, The State University of New Jersey.

References

[1] K. McNamara and S. A. M. Tofail, "Nanoparticles in biomedical applications," *Adv. Phys. X*, vol. 2, no. 1, pp. 54–88, Jan. 2017, doi: 10.1080/23746149.2016.1254570.

[2] W. Li *et al.*, "Microfluidic fabrication of microparticles for biomedical applications," *Chem. Soc. Rev.*, vol. 47, no. 15, pp. 5646–5683, 2018, doi: 10.1039/C7CS00263G.

[3] A. Kaur, O. Shimoni, and M. Wallach, "Novel screening test for celiac disease using peptide functionalised gold nanoparticles," *World J. Gastroenterol.*, vol. 24, no. 47, pp. 5379–5390, Dec. 2018, doi: 10.3748/wjg.v24.i47.5379.

[4] N. Mustafaoglu, T. Kiziltepe, and B. Bilgicer, "Site-specific conjugation of an antibody on a gold nanoparticle surface for one-step diagnosis of prostate specific antigen with dynamic light scattering," *Nanoscale*, vol. 9, no. 25, pp. 8684–8694, 2017, doi: 10.1039/C7NR03096G.

[5] L. Gomez, V. Sebastian, S. Irusta, A. Ibarra, M. Arruebo, and J. Santamaria, "Scaled-up production of plasmonic nanoparticles using microfluidics: from metal precursors to functionalized and sterilized nanoparticles," *Lab Chip*, vol. 14, no. 2, pp. 325–332, 2014, doi: 10.1039/C3LC50999K.

[6] B. Lin, Ed., *Microfluidics: Technologies and Applications*, vol. 304. in Topics in Current Chemistry, vol. 304. Berlin, Heidelberg: Springer Berlin Heidelberg, 2011. doi: 10.1007/978-3-642-23050-9.

[7] W. Buchegger, C. Wagner, B. Lendl, M. Kraft, and M. J. Vellekoop, "A highly uniform lamination micromixer with wedge shaped inlet channels for time resolved infrared spectroscopy," *Microfluid. Nanofluidics*, vol. 10, no. 4, pp. 889–897, Apr. 2011, doi: 10.1007/s10404-010-0722-0.

[8] C. Y. Lim, Y. C. Lam, and C. Yang, "Mixing enhancement in microfluidic channel with a constriction under periodic electro-osmotic flow," *Biomicrofluidics*, vol. 4, no. 1, p. 014101, Mar. 2010, doi: 10.1063/1.3279790.

[9] B. Xu, T. N. Wong, N.-T. Nguyen, Z. Che, and J. C. K. Chai, "Thermal mixing of two miscible fluids in a T-shaped microchannel," *Biomicrofluidics*, vol. 4, no. 4, p. 044102, Dec. 2010, doi: 10.1063/1.3496359.

[10] G. Yesiloz, M. S. Boybay, and C. L. Ren, "Effective Thermo-Capillary Mixing in Droplet Microfluidics Integrated with a Microwave Heater," *Anal. Chem.*, vol. 89, no. 3, pp. 1978–1984, Feb. 2017, doi: 10.1021/acs.analchem.6b04520.

[11] T.-D. Luong, V.-N. Phan, and N.-T. Nguyen, "High-throughput micromixers based on acoustic streaming induced by surface acoustic wave," *Microfluid. Nanofluidics*, vol. 10, no. 3, pp. 619–625, Mar. 2011, doi: 10.1007/s10404-010-0694-0.

[12] N. H. An Le *et al.*, "Ultrafast star-shaped acoustic micromixer for high throughput nanoparticle synthesis," *Lab. Chip*, vol. 20, no. 3, pp. 582–591, 2020, doi: 10.1039/C9LC01174A.

[13] M. Campisi, D. Accoto, F. Damiani, and P. Dario, "A soft-lithographed chaotic electrokinetic micromixer for efficient chemical reactions in lab-on-chips," *J. Micro-Nano Mechatron.*, vol. 5, no. 3–4, pp. 69–76, Dec. 2009, doi: 10.1007/s12213-010-0024-3.

[14] S. A. Vasilescu, S. R. Bazaz, D. Jin, O. Shimoni, and M. E. Warkiani, "3D printing enables the rapid prototyping of modular microfluidic devices for particle conjugation," *Appl. Mater. Today*, vol. 20, p. 100726, Sep. 2020, doi: 10.1016/j.apmt.2020.100726.

[15] E. Tóth, E. Holczer, K. Iván, and P. Fürjes, "Optimized Simulation and Validation of Particle Advection in Asymmetric Staggered Herringbone Type Micromixers," *Micromachines*, vol. 6, no. 1, pp. 136–150, Dec. 2014, doi: 10.3390/mi6010136.

[16] J. Ortega-Casanova and P. Benitez-Alcaide, "Micromixing Enhancement by Optimizing the Geometry of a Micromixer by Means of Response Surface Methodology: Application to Chemical Microreactors," *Micro Nanosyst.*, vol. 9, no. 1, Nov. 2017, doi: 10.2174/1876402909666170705110931.

[17] J. Ortega-Casanova and C.-H. Lai, "CFD study about the effect of using multiple inlets on the efficiency of a micromixer. Assessment of the optimal inlet configuration working as a microreactor," *Chem. Eng. Process. - Process Intensif.*, vol. 125, pp. 163–172, Mar. 2018, doi: 10.1016/j.cep.2018.01.017.